DOI: 10.1002/ejic.201100639

Photophysical and Electrochemical Properties of Phenanthroline-Based Bis-cyclometallated Iridium Complexes in Aqueous and Organic Media

Reshmi V. Kiran,[a] Conor F. Hogan,*[a] Bruce D. James,[a][‡] and David J. D. Wilson[a]

Keywords: Iridium / Electrochemistry / Luminescence / Density functional calculations

The electrochemical and photophysical properties of bis-cyclometallated iridium(III) complexes containing phenanthroline-based ligands have been investigated and compared in organic and aqueous media. Complexes having general formula $[Ir(ppy)_2(\widehat{NN})]^{+/-}$ were synthesized, where ppy is the cyclometallating ligand, 2-phenylpyridine, and $\widehat{NN}$ represents one of the following phenanthroline based ligands: 1,10-phenanthroline (phen), 4,7-diphenyl-1,10-phenanthroline (dpp) and 4,7-diphenyl-1,10-phenanthrolinedisulfonate (BPS). In the case of $[Ir(ppy)_2(BPS)]^-$, the SO_3^- group located on the phenyl ring of BPS dramatically increases the aqueous solubility of the complex compared to the dpp complex, which is only soluble in organic media. The chloride salt of the underivatized phen complex, though not as soluble as the BPS chelated complex, is sufficiently soluble (> 1 mM) for sensing and other applications in aqueous media. The electrochemical response depends markedly on the medium; all the complexes showed reversible behaviour in organic media, whereas the oxidative electrochemistry of $[Ir(ppy)_2BPS]^-$ and $[Ir(ppy)_2phen]^+$ was irreversible. Results from spectroelectrochemical experiments indicate that electrolysis produces significant changes to the UV region of the spectrum associated with the ppy moieties. Significantly, this demonstrates that the highest occupied molecular orbital (HOMO) is not entirely metal based but is also associated with the cyclometallating ligand. The variation in emission maxima between the iridium complexes was small in organic and aqueous media, but the colour of the emission depends on solvent polarity and strongly on temperature. Most significantly, the quantum yields for these species are also strongly influenced by the solvent: high quantum yields, ranging from 14.0 to 28.6 %, are observed in CH_2Cl_2. However, in aqueous media the water-soluble complexes, $[Ir(ppy)_2BPS]^-$ and $[Ir(ppy)_2phen]^+$, exhibited significantly diminished quantum yields of 2.5 and 2.6 %, respectively. Theoretical calculations confirm the spectroscopic assignments and that the HOMO is significantly delocalized over the metal and cyclometallating ligands. The relationship between the electrochemical, spectroscopic and theoretical results is discussed.

Introduction

Luminescent cyclometallated iridium complexes have captured the interest of many scientists, principally as triplet emitters in organic light emitting diode devices,[1–7] and increasingly for potential applications in biological and chemical sensing[8] and bioimaging.[9]

Due to strong spin–orbit coupling promoted by the heavy metal centre,[10] charged heteroleptic and neutral homoleptic iridium complexes often exhibit high quantum yields and long excited state lifetimes in organic media. Bis-cyclometallated complexes of the general formula $[Ir(\widehat{CN})_2(\widehat{NN})]^+$, where $\widehat{CN}$ is a cyclometallating ligand and $\widehat{NN}$ is a chelating diimine ligand, have received considerable interest. The $\widehat{CN}$ ligand is commonly a 2-phenylpyridine (ppy) derivative, whereas $\widehat{NN}$ is typically based on 2,2′-bipyridine (bpy), 1,10′-phenanthroline (phen) or structurally similar ligands. For example, $[Ir(ppy)_2phen]^+$ has been reported to produce coreactant electrochemiluminescent (ECL) emission four times more intense than $[Ru(bpy)_3]^{2+}$ in acetonitrile.[11] Photoluminescent quantum yields of up to 0.43 have been reported for a range of such complexes containing phen ligands suitably derivatized for bioconjugation.[12] $[Ir(ppy)_2dpp]^+$, where dpp is 4,7-diphenyl-1,10-phenanthroline, has been shown to be highly emissive and to have promising electroluminescent properties.[13]

Although the photochemical properties of iridium complexes have been the subject of intensive investigation in recent years, their behaviour in aqueous media remains largely unexplored. This is an undesirable situation because many of the proposed applications for these materials are based in aqueous media. A series of water-soluble iridium(III) bis-terpyridine complexes has been recently synthesized by Williams et al., some of which display high intensity and extremely long-lived emission in aqueous solution.[8d,14] Konishi et al. have described the synthesis and photophysical properties of a tris-cyclometallated iridium(III) complex bearing the bulky ligand 3′,5′-bis(4-

[a] Department of Chemistry, La Trobe Institute for Molecular Science, La Trobe University,
Victoria 3086, Australia
E-mail: c.hogan@latrobe.edu.au
[‡] Deceased on July 8, 2009; this paper is dedicated to his memory.
Supporting information for this article is available on the WWW under http://dx.doi.org/10.1002/ejic.201100639.

carboxylphenyl)-3-(2-pyridyl)biphenyl-4-yl, which has the potential for sensing heavy metals such as lead, cadmium and mercury.[15] Lo et al. have described the properties of a series of bis-cyclometallated iridium complexes containing biotin-derivatized bipyridine ligands. Some photophysical properties in mixed aqueous/organic media have been reported, and the application of the complexes in live cell imaging has been demonstrated.[16] The most substantial study to date on the luminescent properties of cyclometallated iridium complexes in aqueous media is that of Jiang et al.[17] In a study focused on cell imaging applications, the authors have reported a series of bis-cyclometallated complexes with an ancillary ligand of the zwitterionic diimine 4-carboxy-2,2′-bipyridine-4′-carboxylate, with variation of the cyclometallating ligands.

Apart from the aforementioned work, there has been little detailed study into the photophysical properties and virtually no investigation of the electrochemical properties of bis-cyclometallated heteroleptic iridium(III) complexes in pure aqueous media. Our group has recently reported the analytically useful chemiluminescence of the new bathophenanthroline sulfonate (BPS) complex, $[Ir(ppy)_2BPS]Cl$, as well as the related $[Ir(ppy)_2phen]Cl$ and $[Ir(ppy)_2bpy]Cl$ (bpy = bipyridine) in aqueous solution.[8a] In this contribution we present the first full electrochemical and photophysical characterization of phen-based bis-cyclometallated iridium(III) complexes in both organic and aqueous media. The water-soluble complexes $[Ir(ppy)_2BPS]^-$ and $[Ir(ppy)_2phen]^+$ are compared with $[Ir(ppy)_2dpp]^+$,which is only soluble in organic media. Our interest in these materials is driven by potential sensing applications related to their chemiluminescent, electrochemiluminescent and photoluminescent properties. Our results provide insights into the nature of the charge transfer (CT) leading to the excited state in this class of complex.

Results and Discussion

Synthesis

The synthesis of the iridium complexes was carried out in two steps. The dichloro-bridged dimer was synthesized using a modification of a procedure by Sprouse.[18] The iridium complexes were obtained by cleaving the chloride bonds of the dimer with the corresponding diimine ligands (phen, dpp or BPS) as shown in Scheme 1 for the BPS complex. These reactions require mild conditions, and products were obtained in high yields. One or both of column purification and recrystallization was required to obtain pure products. All complexes were characterized using 1D (^1H, ^{13}C) and 2D NMR (COSY, DEPT, heteronuclear single quantum coherence). ESI mass spectrometry and elemental analysis were also carried out. The positions of the sulfonate groups are not specified for commercially available BPS; NMR spectroscopy revealed that the sulfonate groups are located in the *meta* positions on the phenyl rings rather than the *para*, which is often assumed. $[Ir(ppy)_2BPS]Cl$ exists as a chloride salt in the solid state because the sulfonate groups each retain a sodium cation. In solution, the complex exists as $[Ir(ppy)_2BPS]^-$ (see Supporting Information, Figures S1–S10 for its characterization).

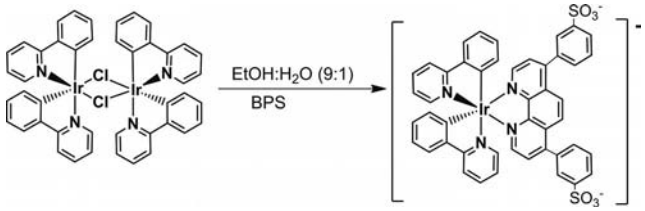

Scheme 1. Synthesis of $[Ir(ppy)_2BPS]^-$.

Electrochemistry

The electrochemical properties of the bis-cyclometallated iridium(III) complexes were investigated in both organic and aqueous media using cyclic voltammetry. The results for the complexes in CH_2Cl_2 and aqueous solution are summarized in Table 1. Due to the limited cathodic potential window of CH_2Cl_2, in some cases redox potential data in CH_3CN are also presented.

Table 1. Formal potentials ($E°$) in aqueous and CH_2Cl_2 media, and excited state redox potentials (E^*) for the complexes studied. Values in parenthesis represent quasi- or irreversible peaks. Data for $[Ru(bpy)_3]^{2+}$ are included for comparison.

	Aqueous $E°$ [V] (vs. Ag/AgCl)	Organic[c] $E°$ [V] (vs. ferrocene)				
Complex	$Ir^{3+/4+}$	$Ir^{3+/4+}$	$\widehat{NN}$	ppy	E^*_{ox}[f]	E^*_{red}[f]
$[Ir(ppy)_2BPS]^-$	(1.10)[a]	0.89	–1.81	–	–1.41	0.50
$[Ir(ppy)_2phen]^+$	(1.08)[b]	0.90	(–1.83)	(–2.52)[d]	–1.61	0.58
$[Ir(ppy)_2dpp]^+$	–	0.86	–1.84	(–2.42)[d]	–1.49	0.51
$[Ir(ppy)_2Cl]_2$	–	0.53, 0.80[e]	–	–	–	–
$[Ru(bpy)_3]^{2+}$	1.08	0.98	–1.72, –1.97	–	–1.15	0.41

[a] 0.1 M $LiClO_4$, 5 mM complex. [b] Phosphate buffer (0.2 M), 1 mM complex. [c] In CH_2Cl_2/0.2 M $TBAPF_6$, 1 mM complex. [d] In CH_3CN/0.2 M $TBAPF_6$, 1 mM complex. [e] A single redox couple is observed at 0.6 V vs. Fc in acetonitrile (see Supporting Information). [f] Excited state redox potentials estimated using $E^*_{ox} = E°(A^+/A) - E^{0-0}$ and $E^*_{red} = E°(A/A^-) + E^{0-0}$, where $E°(A^+/A)$ and $E°(A/A^-)$ are the ground state redox potentials and the E^{0-0} energy is estimated from the low-temperature emission data in Table 3.

The cyclic voltammetric responses for $[Ir(ppy)_2BPS]^-$, $[Ir(ppy)_2phen]^+$ and $[Ir(ppy)_2dpp]^+$ dissolved in CH_2Cl_2 are presented in Figure 1. In organic media the electrochemical responses of the three complexes are characterized by a single reversible oxidative wave between 0.86 and 0.90 V vs. ferrocene. This may be formally attributed to the oxidation of the iridium metal centre $[Ir^{3+/4+}]$ although, as will be discussed later, the molecular orbital associated with this process is significantly distributed over other parts of the complex. The phen complex also shows an irreversible wave due to the oxidation of its chloride counterion. In the range of –1.81 to –1.84 V vs. ferrocene, a single wave is observed for

each complex, which is attributed to the one-electron reduction of the $\widehat{NN}$ ligand.[8b,12,19] In CH_3CN, $[Ir(ppy)_2dpp]^+$ and $[Ir(ppy)_2phen]^+$ exhibit similar patterns to those observed in CH_2Cl_2. The larger potential window available in CH_3CN allowed the observation of a further quasi-reversible redox couple at more negative potentials of –2.42 and –2.52 V for $[Ir(ppy)_2dpp]^+$ and $[Ir(ppy)_2phen]^+$, respectively (Figures S11 and S12, Supporting Information). These are attributed to the reduction of the cyclometallating ppy ligands, which is known to occur at a more negative potential than diimine ligands.[12,19c,20] We were unable to make a similar observation for $[Ir(ppy)_2BPS]^-$ due to its limited solubility in CH_3CN.

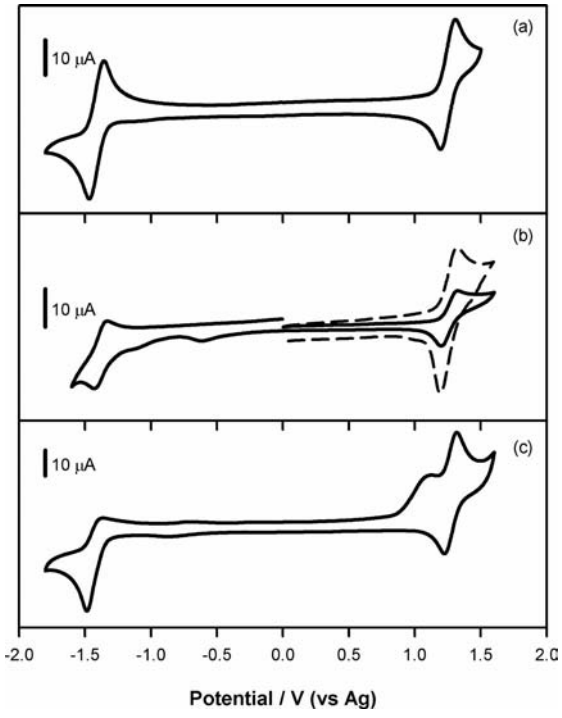

Figure 1. Cyclic voltammetry of (a) $[Ir(ppy)_2dpp]^+$, (b) $[Ir(ppy)_2BPS]^-$ and (c) $[Ir(ppy)_2phen]^+$ in CH_2Cl_2 containing 0.2 M $TBAPF_6$. The concentration was 1 mM in each case, a 3 mm diameter glassy carbon (GC) electrode was used in (a) and (c) and a 2 mm diameter platinum electrode was used in (b). The main scan in each case was run at 0.2 $V s^{-1}$, (b) shows an additional scan (dashed line) run at 1.0 $V s^{-1}$.

The response for $[Ir(ppy)_2BPS]^-$ at the faster scan rate of 1.0 $V s^{-1}$ in the positive region of the voltammogram is also shown in Figure 1. The narrowing of the return wave and the fact that it becomes more prominent with increasing scan rate (Figure S13, Supporting Information) is consistent with the complex being weakly adsorbed in the neutral (oxidized) state.[21] Repeated cycling (> 10 cycles) results in some build up of material on the electrode, which eventually blocks the surface and results in diminished current. Despite this, the redox potentials obtained from the initial scans should approximate the pure solution phase values at slow scan rates well.[22]

For comparison, the electrochemistry of the dimeric starting material was investigated under the same conditions. As previously noted,[23] the dimer remains intact in weakly coordinating CH_2Cl_2 where two redox waves were observed at 0.53 and 0.80 V vs. ferrocene corresponding to the oxidation of the two iridium centres. No other waves were observed for the dimer within the potential window of this solvent, however several irreversible processes corresponding to the reduction of the ppy ligands were noted in CH_3CN solvent at more negative potentials. Moreover, in CH_3CN one reversible $Ir^{3+/4+}$ voltammetric wave was observed at the positive end of the voltammogram rather than two. This is a result of cleavage of the dimer to form a solvent-coordinated mononuclear complex $[Ir(ppy)_2(CH_3CN)Cl]$[23] (Figure S14, Supporting Information).

In aqueous media the electrochemical behaviour of the two water-soluble iridium complexes, $[Ir(ppy)_2BPS]^-$ and $[Ir(ppy)_2phen]^+$, is substantially different from that observed in the organic solvents (Figure 2). As in the organic solvents, a voltammetric signal is observed above 1.0 V vs. Ag/AgCl in each case, {1.08 and 1.10 V for $[Ir(ppy)_2phen]^+$ and $[Ir(ppy)_2BPS]^-$, respectively}. However, unlike those in organic solution, in aqueous media the waves are irreversible or quasi-irreversible in nature. The ligand reductions are not observed in water as only the positive region of the potential scale is accessible. It is interesting to note that the reversibility of the oxidative wave due to $[Ir(ppy)_2BPS]^-$ increases with increasing scan rate. The plot on the right in Figure 2 illustrates the response for the BPS complex in aqueous solution at 0.05 and at 1 V/s. At the faster scan rate the return peak for the rereduction of the complex is more prominent. No such scan rate dependence was observed for $[Ir(ppy)_2phen]^+$ up to 50 V/s. Although the proximity of the redox waves to the solvent limit precluded sensible kinetic analysis by modelling or other means, it is clear that the process responsible for the observed chemical irreversibility in these systems is more rapid in $[Ir(ppy)_2phen]^+$. In $[Ir(ppy)_2BPS]^-$, the process is sufficiently slow to be manifested on the cyclic voltammetric timescale.

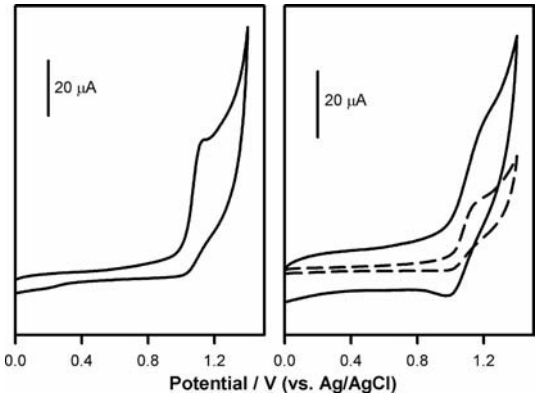

Figure 2. Aqueous cyclic voltammetry of the water-soluble iridium complexes using a 3 mm diameter GC electrode. 1 mM $[Ir(ppy)_2phen]^+$ at 0.2 $V s^{-1}$ in 0.2 M phosphate buffer (left) and 5 mM $[Ir(ppy)_2BPS]^-$ in 0.1 M $LiClO_4$ at 0.05 and 1.0 $V s^{-1}$ (right).

Absorption Spectroscopy

The UV/Vis absorption spectra of $[Ir(ppy)_2phen]^+$ and $[Ir(ppy)_2BPS]^-$ in H_2O and that of $[Ir(ppy)_2dpp]^+$ in CH_2Cl_2 are illustrated in Figure 3 (see Figure S15 in Supporting Information for raw spectra). The electronic absorption spectroscopic data in both solvents (where solubility allows) are summarized in Table 2. Solvent polarity (CH_2Cl_2 vs. H_2O) does not influence the positions of the absorption bands. For cyclometallated iridium(III) diimine systems, intense absorption bands below 320 nm are assigned to spin allowed π–π* ligand-centred (LC) transitions that occur in the cyclometallated ppy and the $\widehat{NN}$ phen-based ligands.

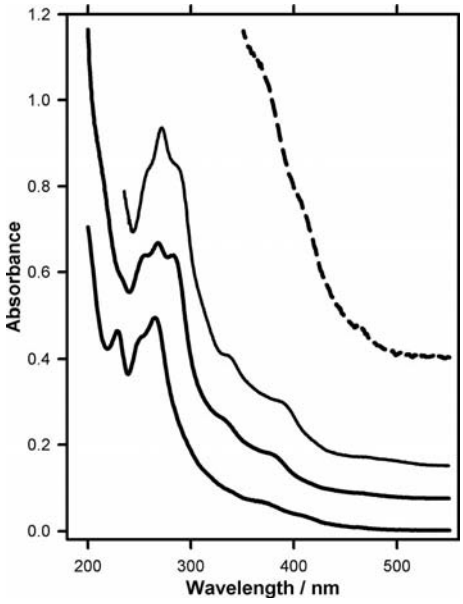

Figure 3. Absorbance spectra of 10 μM $[Ir(ppy)_2phen]^+$ (bottom) and $[Ir(ppy)_2BPS]^-$ (middle) in H_2O and $[Ir(ppy)_2dpp]^+$(top solid line) in CH_2Cl_2 (spectra offset for clarity). The upper dashed curve shows an expanded view of the visible region of the $[Ir(ppy)_2phen]^+$ spectrum.

Table 2. Absorbance data for the iridium complexes in CH_2Cl_2 and H_2O at 298 K.

Complex	Solvent	λ_{abs} [nm] ($\varepsilon \times 10^4$ [M^{-1} cm^{-1}])
$[Ir(ppy)_2phen]^+$	CH_2Cl_2	253(4.6), 264(4.7), 333(1.0), 381(0.8), 411(0.4), 450(0.1), 461(0.1)
	H_2O	252(4.5), 264(4.7), 333(1.0), 367(0.7), 411(0.4), 450(0.1), 453(0.1)
$[Ir(ppy)_2dpp]^+$	CH_2Cl_2	256(3.4), 270(3.9), 286(3.5), 334(1.3), 387(0.8), 450(0.1), 466(0.1)
$[Ir(ppy)_2BPS]^-$	CH_2Cl_2	256(6.0), 270(6.4), 285(6.1), 333(2.4), 386(1.4), 450(0.2), 466(0.2)
	H_2O	252(5.6), 265(5.8), 279(5.6), 329(1.9), 373(1.1), 412(0.3), 450(0.2), 455(0.1)

Although the two types of ligand on these complexes are structurally similar, they are electronically diverse, and it is well established that the energy of the lowest unoccupied molecular orbital (LUMO) for the cyclometallated (anionic) ligand is expected to be higher than that of an isoelectronic but neutral polypyridine ligand. In particular, on the basis of data for similar complexes,[19a,24] the bands peaking at wavelengths less than 270 nm are assigned to ppy-centred transitions, whereas absorption in the 270–300 nm range is attributed to the diimine ligand. A well-defined peak is seen at approximately 285 nm for the two diphenylphen complexes, which is absent for the unsubstituted phen complex. Therefore, this is assigned to a π–π* transition centred on the phenyl rings of the diimine ligands. In accordance with the literature,[3,19c,20a,25] the less intense absorption bands observed at lower energy (320–440 nm) are attributed to a spin allowed CT transition where CT occurs from the HOMO to a phen-ligand based π* orbital. The correct assignment of these bands as metal-to-ligand MLCT [dπ(Ir)→π*(phen)] or ligand-to-ligand LLCT bands [π(ppy)→π*(phen)][17,19a] depends on the nature of the HOMO and the extent to which it is delocalized over the metal and the ppy ligand. The very weak absorption bands above 440 nm are the result of spin forbidden CT transitions, which are more pronounced in iridium complexes compared to analogous ruthenium complexes due to heavy metal induced spin–orbit coupling.

Spectroelectrochemistry

The changes observed in the absorption spectra of $[Ir(ppy)_2phen]^+$ in CH_2Cl_2 over a period of ca. 10 min as the solution is oxidized using a Pt gauze working electrode biased at 1.25 V vs. Ag/AgCl are depicted in Figure 4. Only

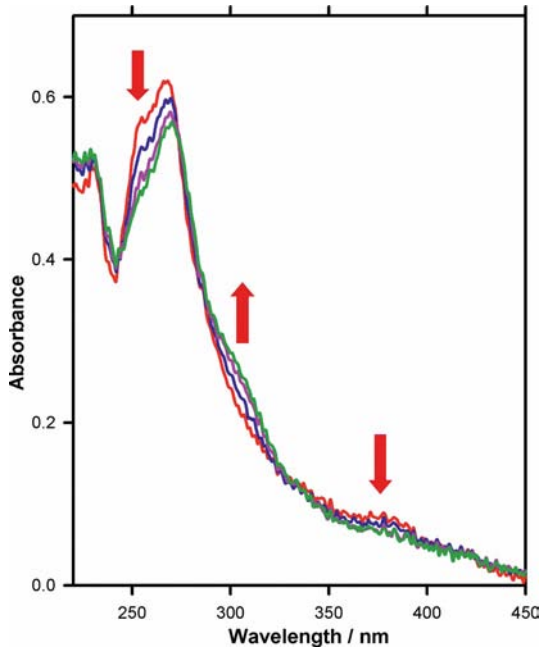

Figure 4. UV/Vis spectroelectrochemical response for 1×10^{-4} M $[Ir(ppy)_2phen]^+$ in CH_2Cl_2 containing 0.1 M $TBAPF_6$, with the oxidation potential held constant at 1.25 V using a Pt gauze electrode in a thin layer cell. The arrows indicate the direction of change in peak magnitudes over the course of the experiment (≈ 10 min).

relatively minor changes are evident in the visible region of the spectrum on electrolysis of the solution. This is in contrast to the situation with complexes such as $[Ru(bpy)_3]^{2+}$ or $[Ru(phen)_3]^{2+}$ where a MLCT band at 460 nm is lost completely on oxidation of the metal centre from the 2+ to the 3+ state.[26] The most significant change to the spectrum of the iridium complex on oxidation is the loss of the band at 253 nm, which is assigned to a $\pi\rightarrow\pi^*$ ppy (LC) transition. This change is observed in both dichloromethane and water (Figure S16, Supporting Information). Although the peak substantially returns on stepping the potential to a more reducing value (0.5 V) in CH_2Cl_2, in aqueous solution the loss is irreversible.

Clearly, oxidation of the complex results in changes to a MO closely associated with ppy. These observations strongly suggest that the HOMO in these complexes is appreciably associated with a cyclometallated ligand and not simply the metal centre. Moreover, reversible electrochemistry observed in organic media should not be taken as evidence of a purely metal-based redox orbital. These observations have implications for the assignment of the CT transitions leading to the excited state in these complexes.

Photoluminescence

All three complexes exhibit intense photoluminescence under the conditions used in this study. Specifically, in dichloromethane, water and alcohol (1:4 EtOH/MeOH) at ambient temperatures and in alcohol glass at 77 K. Photoluminescence data are summarized in Table 3, which includes the corresponding data for $[Ru(bpy)_3]^{2+}$ (a pure MLCT emitter) obtained under the same conditions for comparative purposes. In organic media, the values of the photoluminescent quantum yields (Φ_p) decrease in the order $[Ir(ppy)_2BPS]^- > [Ir(ppy)_2dpp]^+ > [Ir(ppy)_2phen]^+ > [Ru(bpy)_3]^{2+}$. The high intensity of the luminescence in dichloromethane is evidenced by large values of Φ_p, which range from 14.0–28.6%, compared to 4.2% for $[Ru(bpy)_3]^{2+}$ in the same medium. However, in aqueous media the quantum yields for the iridium complexes are significantly reduced and the order is reversed with both $[Ir(ppy)_2phen]^+$ (2.6%) and $[Ir(ppy)_2BPS]^-$ (2.5%) being outperformed by the ruthenium standard (4.2%).

Little variation was observed in the wavelength of the maximum emission between the three phen-based iridium complexes in the same media. For example, in CH_2Cl_2, λ_{max} ranged between 583 and 587 nm, the results in alcohol and water being similarly invariant (see Table 3). These observations parallel the electrochemical data presented earlier, where the oxidation and first reduction formal potentials (E^0) were similar for each complex.

A noteworthy observation is the solvatochromism displayed by these complexes at ambient temperatures, where the emission maxima are found to be dependant on the polarity of the solvent.

The emission spectra of $[Ir(ppy)_2BPS]^-$ in dichloromethane and water are plotted in Figure 5 (a). The significant solvatochromic redshift with increased solvent polarity, and the distinct broadening of the spectrum in water apparent in Figure 5 (a) are indicative of a CT excited state where substantial charge separation exists. As illustrated in Figure 5 (b), each of the iridium complexes displays a bathochromic shift when excited in more polar solvents such as EtOH/MeOH and H_2O compared with dichloromethane. Because the polarities of the complexes at ground and excited state are substantially different; a change in the solvent polarity leads to greater stabilization. This results in a change in energy gap between these electronic states, which results in a shift of the energies of the emission maxima.

The photoluminescent spectra of all three iridium complexes are illustrated in Figure 5 (c), both in fluid alcoholic medium at 298 K and in a 77 K alcohol glass. There is a significant blueshift apparent for the complexes at low temperature compared to the ambient temperature spectra. Moreover, whereas the room temperature spectra are broad and featureless, the spectra in 77 K alcohol glass display structure. A blueshift at low temperature is typical of CT states and its magnitude is related to the degree of charge separation between the ground and excited states. $[Ru(bpy)_3]^{2+}$, which is regarded as a typical MLCT emitter, displays a shift of 948 cm^{-1} under the conditions used here, and analogous ruthenium and osmium complexes are

Table 3. Photophysical properties of iridium complexes in various media.

Complex	Solvent	λ_{max} [nm]	Φ_p[c] (aerated)	Φ_p[c] (degassed)
$[Ir(ppy)_2phen]Cl$[e]	CH_2Cl_2	584	0.045[a]	0.140[a]
	H_2O	605	0.019[a]	0.026[a]
	EtOH/MeOH	594		
	EtOH/MeOH (77 K)	515, 534		
$[Ir(ppy)_2dpp]Cl$[d]	CH_2Cl_2	587	0.078[b]	0.344[b]
	EtOH/MeOH	602		
	EtOH/MeOH (77 K)	528, 555		
$[Ir(ppy)_2BPS]Cl$	CH_2Cl_2	583	0.113	0.286
	H_2O	616	0.023	0.025
	EtOH/MeOH	605		
	EtOH/MeOH (77 K)	537, 564		
$[Ru(bpy)_3]^{2+}$	CH_2Cl_2	606	0.028[b]	0.042[b]
	H_2O	623	0.028[a]	0.042[a]
	EtOH/MeOH	616		
	EtOH/MeOH (77 K)	581, 626, 694		

[a] Chloride salt. [b] PF_6 salt. [c] Quantum yields measured using $Ru(bpy)_3^{2+}$ as the reference and 450 nm as the excitation wavelength. [d] Various quantum yields have previously been reported for $[Ir(ppy)_2dpp]^+$ {Φ in CH_2Cl_2 = 20%, using coumarin 540 as the standard;[27] Φ in CH_3CN = 18.2%, using $[Ir(ppy)_2(bpy)]PF_6$ as the standard;[2a] Φ in CH_3CN = 53%, using $[Ru(4,7\text{-diphenyl-}1,10\text{-phen})_3]Cl_2$ as the standard}.[13] [e] Various quantum yields have previously been reported for $[Ir(ppy)_2phen][PF_6]$ {Φ in CH_2Cl_2 = 7%, using coumarin 540 as the standard;[27] Φ in CH_3CN = 11.9%, using $[Ir(ppy)_2(bpy)]PF_6$ as the standard;[2a] Φ in CH_2Cl_2 = 14%, using Rhodamine 6G as the standard}.[11]

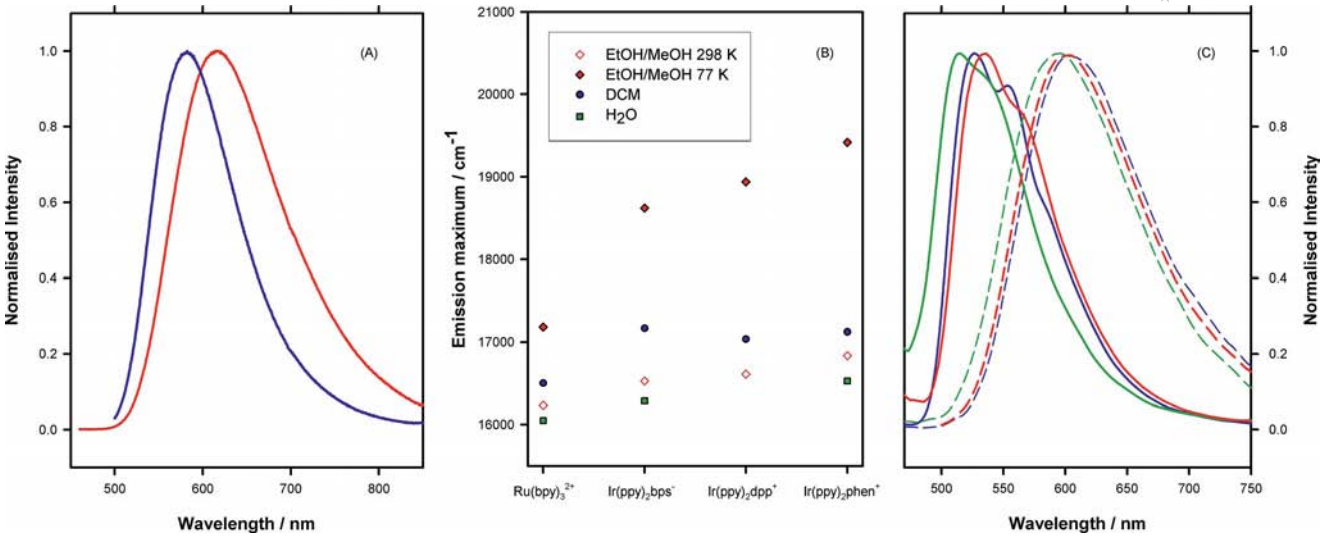

Figure 5. Effect of medium on photoluminescence of iridium complexes. (A) Emission spectra of $[Ir(ppy)_2BPS]^-$ at 298 K in CH_2Cl_2 (blue) and H_2O (red). (B): Effect of medium on photoluminescent emission energy of the three iridium complexes compared with $[Ru(bpy)_3]^{2+}$ in H_2O, CH_2Cl_2, 1:4 EtOH/MeOH solution at 298 K and 1:4 EtOH/MeOH glass at 77 K. (C): Emission spectra of $[Ir(ppy)_2phen]^+$ (green), $[Ir(ppy)_2dpp]^+$ (blue) and $[Ir(ppy)_2BPS]^-$ (red) in 4:1 EtOH/MeOH glass at 77 K (spectra on the left) and in fluid 4:1 EtOH/MeOH solution at 298 K (dashed lines).

known to display shifts of typically no more than 2000 cm^{-1}. The magnitude of the blueshifts observed for the iridium complexes studied here (2093–2582 cm^{-1}) are significantly larger than that expected for a MLCT state. These observations are consistent with an excited state with substantial LLCT character.

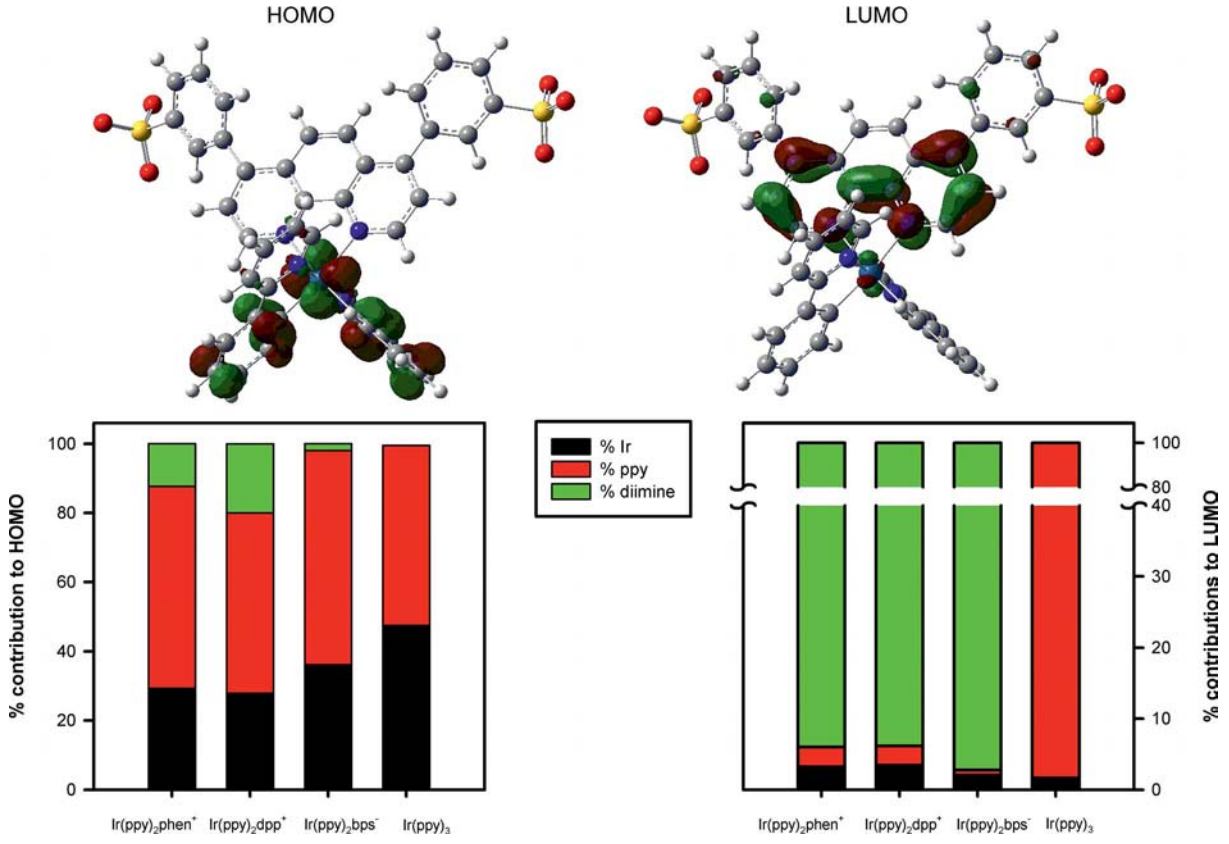

Figure 6. Electron-density maps of frontier MOs in $[Ir(ppy)_2(BPS)]^-$ (top). MO contributions to HOMO and LUMO for each iridium complex (bottom).

Theoretical Calculations

As expected from the electrochemical and spectroscopic data, the nature of the phen-type ligand has only a small effect on the nature of the frontier MOs of the complex. Very similar properties and topologies are found for the HOMO and LUMO of each iridium complex as illustrated in Figure 6. In each case the HOMO comprises contributions from both the iridium atom (30–40%) and the phenyl (π) ring of the ppy ligands (50–60%). The delocalization of the HOMO of these complexes is consistent with the experimental evidence from spectroelectrochemistry and photoluminescence. In each case the LUMO (and LUMO + 1) is almost exclusively composed of the phen core. The next highest energy MOs (LUMO + 2, LUMO + 3) are associated with delocalized π* orbitals on the ppy ligand. Plots of MO topologies for all complexes, as well as contributions to each MO for frontier MOs, are included in the Supporting Information (Figure S17). The calculated energies of the HOMO, LUMO and HOMO–LUMO gap also exhibit little variability (Table S1, Supporting Information).

The time dependent (TD)-DFT results generally support the assignment of absorption bands from the experimental data. The assignment of transitions as being either pure MLCT or LLCT would not be justified due to the delocalization of the MOs, in particular the HOMO, of these complexes. Moreover, the presence of spin–orbit coupling in heavy metal complexes such as these further obfuscates the separation between singlet and triplet states, as well as CT states.

The absorption bands at lower energy (above 400 nm) are generally associated with a greater degree of MLCT, although inclusion of spin–orbit coupling would be required to accurately model this region of the spectrum. The highest energy bands reported in Table S2 (Supporting Information) correspond to ppy-centred transitions, whereas bands corresponding to transitions to the diimine ligand are slightly lower in energy. This is in agreement with the assignment from the experimental spectra outlined above.

Conclusions

The synthesis and characterization of the luminescent, water-soluble, bis-cyclometallated iridium(III) complex $[Ir(ppy)_2BPS]Cl$ has been described. The electrochemical and photophysical properties of this complex and $[Ir(ppy)_2phen]Cl$ have been investigated in both water and organic media and compared with the properties of $[Ir(ppy)_2dpp][PF_6]$ in an organic medium.

Reversible electrochemical waves are observed for the oxidation of these complexes at positive potentials in organic solvents; however, the same redox couples are irreversible in aqueous media. This is in contrast with complexes such as $[Ru(bpy)_3]^{2+}$ or $[Ru(phen)_3]^{2+}$, for which reversible electrochemistry is observed in both organic and aqueous media.[28] It is also noteworthy that the excited state redox potentials for the iridium complexes (Table 1), as estimated from ground state potentials and low temperature emission data, point to a significant level of photochemical activity for these species compared with $[Ru(bpy)_3]^{2+}$.

Spectroelectrochemical experiments show that the most significant change to the absorption spectrum of $[Ir(ppy)_2phen]^+$ on electrochemical oxidation is the loss of a band at 253 nm assigned to a ppy-based π–π* transition. Mirroring the voltammetric data, the loss of the band, which is irreversible in aqueous media, is recovered in organic solvent on re-reduction. These observations suggest that for such iridium complexes the electron abstracted on oxidation is not from the *d*π orbital, but from an orbital that is largely ligand based.

In the localized MO approximation, oxidation and reduction processes are viewed as metal or ligand centred. For example, in the case of the ruthenium complexes, the metallic nature of the HOMO is clear cut. Such arbitrary classification of electronic transitions and electronically excited states loses its meaning when the states involved cannot be described by localized MO configurations.[29] From an electrochemical standpoint, the implication is that the assignment of the first oxidative couple in these complexes as simply Ir^{3+}/Ir^{4+} is not strictly correct. Similarly, the nature of the CT transition leading to the excited state cannot be defined as MLCT or LLCT from a photochemical perspective and certainly such an assignment should not be made on the basis of the reversibility of the oxidative redox couple in organic solvent.

The dependence of the emission wavelength on solvent polarity and the large blueshifts observed on going from fluid media to low temperature glass support the assignment of the excited state as being significantly LLCT in nature. LLCT states are expected to be more distorted than MLCT states with respect to the ground state. Therefore, relatively higher stabilization occurs in polar solvents and a more significant redshift in emission is observed.

The complexes are highly emissive in organic media but significantly less so in water. For example the photoluminescent quantum yield (Φ_p) for $[Ir(ppy)_2BPS]^-$ plunges from 28.6 to 2.5% on going from CH_2Cl_2 to H_2O. The strong solvent dependence of Φ_p is in contrast with pure MLCT emitters such as $[Ru(bpy)_3]^{2+}$ and is clearly related to the nature of the excited state. This significant effect is likely related to the distorted nature of the excited state, due to its LLCT character, which being more photochemically active, could lead to nonemissive deactivation interactions with polar solvents. This instability is mirrored in the difference in electrochemical reversibility between organic and aqueous media when the electron is removed from the HOMO electrolytically rather than by optical excitation. Based on our observations of other complexes (for example complexes containing a bipyridine based auxiliary ligand), it would appear that the sensitivity of the quantum yields and the electrochemical characteristics is quite general for bis-cyclometallated iridium complexes of this type.

DFT calculations showed that the LUMO in each of the complexes is dominated by the diimine ligand, whereas the

HOMO contains significant contributions from both the metal and the ppy ligands. The metal contributions to the HOMOs are relatively low (≈ 30%) compared to $Ir(ppy)_3$ (≈ 50%). This strongly supports the picture painted by the electrochemical, spectroscopic and spectroelectrochemical data, that the nature of the transition leading to the excited state in these materials is not adequately described as MLCT as it is, to a significant extent, an intraligand transition.

The dependence of the luminescent intensity on solvent polarity has obvious implications for the application of bis-cyclometallated iridium complexes in sensing, which is almost exclusively carried out in aqueous environments. Although such applications are frequently alluded to for this class of iridium complex in the literature, the vast majority of investigations focus exclusively on their properties in organic media. Apart from the luminescence, the irreversible nature of the electrochemistry in aqueous solution has particular ramifications for the application of these materials in ECL-based sensing. Nonetheless, we will show in a subsequent publication that their ECL sensing properties rival those of the dominant ruthenium complexes under some circumstances.

Experimental Section

Chemicals: Tris(2,2′-bipyridyl)ruthenium(II) dichloride hexahydrate, $[Ru(bpy)_3]Cl_2{\cdot}6H_2O$ (> 99%), iridium trichloride hydrochloride hydrate ($IrCl_3{\cdot}xH_2O{\cdot}xHCl$, > 99.9%), 2-phenylpyridine (99.9%), bathophenanthrolinedisulfonic disodium (99.9%), 4,7-diphenyl-1,10-phenanthroline (99.9%), 1,10-phenanthroline (99%), lithium perchlorate ($LiClO_4$, > 99%), sodium chloride (NaCl, 99.5%), dichloromethane (CH_2Cl_2, 99.9%), acetonitrile (CH_3CN, 99.9%) and ethoxyethanol (99%) from Aldrich were employed without further purification, whereas ethanol and methanol were distilled. Potassium Phosphate Dibasic (K_2HPO_4, > 98%) was obtained from May & Baker and Potassium Phosphate Monobasic (KH_2PO_4, > 99%) was purchased from Ajax Chemicals. $[Ru(bpy)_3][PF_6]_2$ was obtained by converting the Cl salt to PF_6 by metathasis. Unless otherwise stated, all solutions were freshly prepared with deionized water (Milli Q, Millipore).

General Characterization: NMR spectra were obtained with a Bruker Avance 300 MHz spectrometer operating at 27 °C. Measurements were carried out in deuterated methanol, deuterated chloroform or deuterium oxide. MS was performed by ionizing the samples in 50:50 water/methanol mixture by ESI with a Finnigan LTQ FT hybrid mass spectrometer (Bremen, Germany) with linear ion trap and Fourier transform ion cyclotron resonance. Elemental Analyses (C, N, H, S, Cl) were obtained by the Campbell Microanalytical Laboratory, University of Otago, New Zealand.

Electrochemistry: Cyclic voltammetry was carried out using a PC-controlled CH660 potentiostat with picoamp booster & faraday cage (CH instruments) or a μ-Autolab Type II (Eco Chemie, Netherlands) electrochemical workstation. A conventional three-electrode cell was used, with platinum 1 cm^2 gauze as the counter electrode. The working electrodes used were disks of different materials (Pt and GC) and different dimensions (3 mm diameter GC and 2 mm diameter Pt) shrouded in Teflon. They were cleaned by polishing with 0.3 μm alumina on a felt pad and sonicating in acetone followed by MQ water for 5 min. For aqueous systems, an Ag/AgCl (3 M KCl) reference electrode was used. In organic solvents, a Ag wire pseudo reference was used, in which case peaks were referenced to the formal potential of ferrocene (0.31 V vs. SCE) measured in situ.[30] Nonaqueous reference electrodes were prepared using the same solvent as in the test solution with the same concentration of electrolyte (0.1 M or 0.2 M $TBAPF_6$). Spectroelectrochemical measurements were made using a 1 mm path length cuvette as the electrochemical cell using a 0.5×0.7 mm platinum gauze as working electrode, platinum counter and Ag wire (quasi-reference electrode) or Ag/AgCl (reference). Solutions were degassed with nitrogen (99.99% Linde) for a minimum of 5 min prior to commencing an experiment. All electrochemical measurements were carried out at 23 ± 5 °C.

Photochemistry: UV/Vis spectra were recorded using a Varian Cary UV/Vis spectrometer. Emission spectra were recorded using a Varian Cary Eclipse fluorescence spectrophotometer. Correction factors from 320–850 nm were determined using a calibrated lamp (Optronic Labs Spectral Irradiance standard OL245M) combined with a constant current power supply (Optronic Labs OL65A). Room temperature measurements were made using 1 cm quartz cells with screw top lids and septa, whereas, for low temperature (77 K) measurements, a 1 cm diameter glass tube cooled with liquid nitrogen was used. The excitation and emission slits were set at 5 nm band pass for all experiments. In determining the emission maxima (λ_{max}) or the area under the emission spectrum, the original spectrum was first corrected for variation in photomultiplier tube (PMT) responsivity with wavelength using the predetermined instrumental correction factors. Quantum yields were determined using the following equation:

$$\Phi_x = \Phi_{ref} (Grad_x/Grad_{ref})(\eta^2{}_x/\eta^2{}_{ref})$$

where Φ_{ref} is the quantum yield of the reference complex, $[Ru(bpy)_3]^{2+}$, whose photoluminescence quantum yield is known to be 0.042 in H_2O[31] and CH_2Cl_2,[11] *Grad* is the gradient of the absorbance vs. integrated emission intensity graph, using at least five different concentrations with absorbance below 0.1 and achieving R^2 close to 1, x denotes sample and ref is the reference and η is the refractive index of the solvent used. Quantum yield determinations were conducted at room temperature (21 ± 3 °C). Solutions were thoroughly degassed with nitrogen in septum-sealed quartz cells prior to measurements.

Computational Methods: DFT calculations were carried out within the Gaussian 09 suite of programs.[32] Ground state geometries were optimized in the absence of solvent with B3LYP[33] and mPW1PW91[34] functionals in conjunction with the 6-31+G(d) basis set[35] for nonmetal atoms and the LANL2DZ basis set and core potential for iridium.[36] Only mPW1PW91 results are presented as it has been shown previously that this functional yields reliable results.[37] Symmetry of the optimized ground state structures is C_2 {$[Ir(ppy)_2phen]^+$} and C_1 {$[Ir(ppy)_2dpp]^+$, $[Ir(ppy)_2BPS]^-$}. Final single-point energy calculations were carried out at the LANL2DZ/6-31+G(d) optimized geometries using the SDD basis and core potential (MWB)[36a,38] for Ir and the TZVP basis set[39] for all other atoms. The polarizable continuum model[40] selfconsistent reaction field was used to model solvent effects at the gas-phase optimized geometries with solvents as dichloromethane and water. HOMO and LUMO energies were calculated using DFT MOs, as well as with TD-DFT[41] using the SDD/TZVP basis sets, which may be expected to yield accurate and reliable LUMO energies. Excitation energies to singlet and triplet excited states were investigated with TD-DFT, with 40 states calculated. SCF convergence criteria of 10^{-8} a.u. was employed throughout. Molecular orbital analysis was carried out with the AOMix program.[42]

Synthesis: The syntheses of $[Ir(ppy)_2Cl]_2$, $[Ir(ppy)_2phen]Cl$ and $[Ir(ppy)_2dpp][PF_6]$ were carried out using modifications of previously published methods.

$[Ir(ppy)_2Cl]_2$: The dimer was synthesized by modifying the procedure reported by Sprouse,[18] which involved reacting iridium trichloride with 2-phenylpyridine and purifying using flash chromatography (silica/dichloromethane) producing an 85% yield. ^{1}H NMR (300 MHz, CD_2Cl_2): δ = 5.89 (d, J = 6.9 Hz, 4 H), 6.62 (t, J = 7.6 Hz, 4 H), 6.80 (t, J = 6.4 Hz, 4 H), 6.83 (t, J = 6.4 Hz, 4 H), 7.57 (d, J = 7.7 Hz, 4 H), 7.80 (t, J = 6.5 Hz, 4 H), 7.94 (d, J = 7.9 Hz, 4 H), 9.23 (d, J = 5.8 Hz, 4 H) ppm. ^{13}C NMR (300 MHz, $CDCl_3$): δ = 118.70, 122.50, 123.60, 129.01, 130.30, 136.60, 144.02, 144.80, 151.50, 168.01 ppm. $C_{44}H_{32}Cl_2Ir_2N_4$ (1072.11): calcd. C 49.29, H 3.01, N 5.23; found C 49.04, H 3.23, N 5.05.

$[Ir(ppy)_2BPS]Cl$: $[Ir(ppy)_2BPS]Cl$ was synthesized using the route shown in Scheme 1. $[Ir(ppy)_2Cl]_2$ (154 mg, 0.14 mmol) and bathophenanthrolinedisulfonic disodium (99.9%, Aldrich) (171 mg, 0.29 mmol) were heated to reflux in 90:10 ethanol/water (150 mL) under nitrogen for 6 h. The mixture, which had changed colour from yellow to luminescent orange, was rotary evaporated to give crude orange crystals. The crude product was purified using a Sephadex LH-20 column (length 10 cm, diameter 2 cm) with a 20:80 mixture of methanol/ethanol. The purified solution was rotary evaporated and the solid recovered. The complex was dried overnight to obtain 84% yield of a bright orange powder, which was characterized using NMR, MS, IR and microanalysis. The complex contains chloride counterions in the solid state because the sulfonate groups retain their sodium counterions. Nonetheless, the complex carries a net negative charge when dissolved in aqueous or organic solution. ^{1}H NMR (300 MHz, CD_3OD): δ = 6.36 (d, J = 7.5 Hz, 2 H), 6.86 (t, J = 7.4 Hz, 2 H), 6.96 (t, J = 7.5 Hz, 4 H), 7.59 (d, J = 6.1 Hz, 2 H, 6-H), 7.62 (s, 2 H), 7.66 (d, J = 4.34 Hz, 2 H), 7.73 (d, J = 5.2 Hz, 2 H8) 7.81 (m, 4 H), 8.02 (m, 4 H), 8.09 (d, J = 8.1 Hz, 2 H, 4-H), 8.09 (s, 2 H), 8.34 (d, J = 5.2 Hz, 2 H, 5-H) ppm. ^{13}C NMR (300 MHz, CD_3OD): δ = 119.31, 121.97, 122.83, 124.32, 125.67, 126.59, 128.53, 129.02, 129.77, 130.91, 131.22, 135.42, 137.94, 143.74, 145.71, 146.97, 148.52, 149.70, 150.16, 167.44, ppm. $C_{46}H_{38}ClIrN_4Na_2O_6S_2{\cdot}2H_2O$ (1080.6 + 36.0): calcd. C 47.01, H 3.46, Cl 3.04, N 4.82, S 5.55; found C 47.50, H 3.46, Cl 3.09, N 4.82, S 5.55. ESI-MS: m/z = 1037.09 $[M - Cl]^+$. IR: $\tilde{\nu}$ 3431 (OH, br.) cm^{-1}.

$[Ir(ppy)_2phen]Cl$: $[Ir(ppy)_2phen]Cl$ was synthesized by using the procedure described by King (similar to Scheme 1).[23] It involved reacting $[Ir(ppy)_2Cl]_2$ with 1,10-phenanthroline in CH_2Cl_2, purifying the product using an ethanolic sephadex LH-20 column, recrystallizing from CH_2Cl_2 and toluene to yield 80% of orange pure product. ^{1}H NMR (300 MHz, $CDCl_3$): δ = 6.41 (d, J = 7.5 Hz, 2 H), 6.93 (t, J = 6.6 Hz, 2 H), 6.99 (t, J = 7.5 Hz, 2 H), 7.10 (t, J = 7.5 Hz, 2 H), 7.33 (d, J = 6.6 Hz, 2 H), 7.76 (m, 4 H), 7.94 (m, 4 H), 8.26 (d, J = 5.0 Hz, 2 H), 8.44 (s, 2 H), 8.97 (d, J = 8.2 Hz, 2 H) ppm. ^{13}C NMR (300 MHz, $CDCl_3$): δ = 119.46, 122.63, 123.08, 124.64, 126.56, 128.89, 130.67, 131.53, 131.66, 137.95, 139.29, 143.39, 146.40, 148.25, 149.32, 150.45, 167.69 ppm. $C_{34}H_{24}ClIrN_4{\cdot}2.5H_2O$ (716.3 + 45.0): calcd. C 53.64, H 3.84, Cl 4.65, N 7.36; found C 53.49, H 3.77, Cl 4.05, N 7.08. ESI-MS: m/z = 681.1 $[M - Cl]^+$.

$[Ir(ppy)_2dpp][PF_6]$: $[Ir(ppy)_2dpp][PF_6]$ was synthesized using a modified procedure from Bolink (Scheme 1).[13] It involved reacting $[Ir(ppy)_2Cl]_2$ with 4,7-diphenyl-1,10-phenanthroline in CH_2Cl_2 before precipitating the product as a PF_6 salt, which was purified further using an ethanolic Sephadex LH-20 column, yielding 80% of orange pure product. ^{1}H NMR (300 MHz, CD_2Cl_2): δ = 6.48 (d, J = 7.5 Hz, 2 H), 6.97 (t, J = 6.6 Hz, 2 H), 7.04 (t, J = 7.5 Hz, 2 H), 7.16 (t, J = 7.5 Hz, 2 H), 7.51 (d, J = 6.0 Hz, 2 H), 7.65 (m, 10 H), 7.75 (d, J = 5.4 Hz, 2 H), 7.82 (m, 4 H), 8.01 (d, J = 8.0 Hz, 2 H), 8.19 (s, 2 H), 8.40 (d, J = 5.4 Hz, 2 H) ppm. ^{13}C NMR (300 MHz, CD_2Cl_2): δ = 119.74, 122.67, 123.11, 124.80, 126.20, 126.72, 129.05, 129.43, 129.54, 129.77, 130.59, 131.65, 135.24, 138.08, 143.75, 147.30, 148.56, 149.72, 150.55, 150.96, 167.73 ppm. $C_{46}H_{32}F_6IrN_4P{\cdot}2H_2O$ (978.0 + 36.0): calcd. C 54.43, H 3.58, N 5.52; found C 54.36, H 3.48, N 5.69. ESI-MS: m/z = 833.2 $[M - PF_6]^+$.

Supporting Information (see footnote on the first page of this article): Further details of the structural characterisation, electrochemical properties, spectroscopic properties and results from theoretical calculations.

Acknowledgments

We would like to acknowledge helpful discussions on this work with Dr. John Christie, La Trobe University. We acknowledge the Australian research council (ARC) for a discovery project (grant number DP1094179). The authors acknowledge support from the National Computational Infrastructure National Facility (NCI-NF), Victorian Partnership for Advanced Computing (VPAC), Victorian Life Science Computing Initiative (VLSCI) and the high-performance computing facility of La Trobe University.

[1] W.-Y. Lai, J. W. Levell, A. C. Jackson, S.-C. Lo, P. V. Bernhardt, I. D. W. Samuel, P. L. Burn, *Macromolecules* **2010**, *43*, 6986–6994.

[2] a) J. I. Goldsmith, W. R. Hudson, M. S. Lowery, T. H. Anderson, S. Bernhard, *J. Am. Chem. Soc.* **2005**, *127*, 7502–7510; b) M. Kirch, J. M. Lehn, J. P. Sauvage, *Helv. Chim. Acta* **1979**, *62*, 1345–1384.

[3] K. K. W. Lo, D. C. M. Ng, C. K. Chung, *Organometallics* **2001**, *20*, 4999–5001.

[4] a) A. P. de Silva, H. Q. N. Gunaratne, T. Gunnlaugsson, A. J. M. Huxley, C. P. McCoy, J. T. Rademacher, T. E. Rice, *Chem. Rev.* **1997**, *97*, 1515–1566; b) J. N. Demas, B. A. DeGraff, *Coord. Chem. Rev.* **2001**, *211*, 317–351; c) W. S. Tang, X. X. Lu, K. M. C. Wong, V. W. W. Yam, *J. Mater. Chem.* **2005**, *15*, 2714–2720; d) Z. H. Lin, Y. G. Zhao, C. Y. Duan, B. G. Zhang, Z. P. Bai, *Dalton Trans.* **2006**, 3678–3684; e) R. P. Brinas, T. Troxler, R. M. Hochstrasser, S. A. Vinogradov, *J. Am. Chem. Soc.* **2005**, *127*, 11851–11862.

[5] a) S. Zanarini, E. Rampazzo, S. Bonacchi, R. Juris, M. Marcaccio, M. Montalti, F. Paolucci, L. Prodi, *J. Am. Chem. Soc.* **2009**, *131*, 14208–14209; b) J. L. Delaney, C. F. Hogan, J. Tian, W. Shen, *Anal. Chem.* **2011**, *83*, 1300–1306.

[6] G. J. Barbante, C. F. Hogan, D. J. D. Wilson, N. A. Lewcenko, F. M. Pfeffer, N. W. Barnett, P. S. Francis, *Analyst* **2011**, *136*, 1329–1338.

[7] C. Ulbricht, B. Beyer, C. Friebe, A. Winter, U. S. Schubert, *Adv. Mater. (Weinheim, Ger.)* **2009**, *21*, 4418–4441.

[8] a) R. V. Kiran, E. M. Zammit, C. F. Hogan, B. D. James, N. W. Barnett, P. S. Francis, *Analyst* **2009**, *134*, 1297–1298; b) Q. Zhao, S. Liu, M. Shi, C. Wang, M. Yu, L. Li, F. Li, T. Yi, C. Huang, *Inorg. Chem.* **2006**, *45*, 6152–6160; c) G. Di Marco, M. Lanza, M. Mamo, I. Stefio, C. Di Pietro, G. Romeo, S. Campagna, *Anal. Chem.* **1998**, *70*, 5019–5023; d) W. Goodall, J. A. G. Williams, *J. Chem. Soc., Dalton Trans.* **2000**, 2893–2895.

[9] J. S.-Y. Lau, P.-K. Lee, K. H.-K. Tsang, C. H.-C. Ng, Y.-W. Lam, S.-H. Cheng, K. K.-W. Lo, *Inorg. Chem.* **2008**, *47*, 708–718.

[10] S. Lamansky, P. Djurovich, D. Murphy, F. Abdel-Razzaq, H. E. Lee, C. Adachi, P. E. Burrows, S. R. Forrest, M. E. Thompson, *J. Am. Chem. Soc.* **2001**, *123*, 4304–4312.

[11] J. Kim, I. Shin, H. Kim, J. Lee, *J. Am. Chem. Soc.* **2005**, *127*, 1614–1615.

[12] K. K.-W. Lo, C.-K. Chung, T. K.-M. Lee, L.-H. Lui, K. H.-K. Tsang, N. Zhu, *Inorg. Chem.* **2003**, *42*, 6886–6898.

[13] H. J. Bolink, L. Cappelli, E. Coronado, M. Gratzel, E. Orti, R. Costa, P. Viruela, M. Nazeerruddin, *J. Am. Chem. Soc.* **2006**, *128*, 14786–14787.

[14] a) J.-P. Collin, I. M. Dixon, J.-P. Sauvage, J. A. G. Williams, F. Barigelletti, L. Flamigni, *J. Am. Chem. Soc.* **1999**, *121*, 5009–5016; b) M. Licini, J. A. G. Williams, *Chem. Commun.* **1999**, 1943–1944.

[15] K. Konishi, H. Yamaguchi, A. Harada, *Chem. Lett.* **2006**, *35*, 720–721.

[16] K. Y. Zhang, K. K. W. Lo, *Inorg. Chem.* **2009**, *48*, 6011–6025.

[17] W. Jiang, Y. Gao, Y. Sun, F. Ding, Y. Xu, Z. Bian, F. Li, J. Bian, C. Huang, *Inorg. Chem.* **2010**, *49*, 3252–3260.

[18] S. Sprouse, K. A. King, P. J. Spellane, R. J. Watts, *J. Am. Chem. Soc.* **1984**, *106*, 6647–6653.

[19] a) F. Neve, M. L. Deda, A. Crispini, A. Bellusci, F. Puntoriero, S. Campagna, *Organometallics* **2004**, *23*, 5856–5863; b) S. Okada, K. Okinaka, H. Iwawaki, M. Furugori, M. Hashimoto, T. Mukaide, J. Kamatani, S. Igawa, A. Tsuboyama, T. Takiguchi, K. Ueno, *Dalton Trans.* **2005**, *9*, 1583–1590; c) P. Didier, I. Ortmans, A. K.-D. Mesmaeker, *Inorg. Chem.* **1993**, *32*, 5239–5245.

[20] a) G. Calogero, G. Giuffrida, S. Serroni, V. Ricevuto, S. Campagna, *Inorg. Chem.* **1995**, *34*, 541–545; b) F. Neve, A. Crispini, S. Serroni, F. Loiseau, S. Campagna, *Inorg. Chem.* **2001**, *40*, 1091; c) M. G. Colombo, A. Hauser, H. U. Gudel, *Inorg. Chem.* **1993**, *32*, 3088–3092; d) K. K.-W. Lo, C.-K. Chung, T. K.-M. Lee, L.-H. Lui, K. H.-K. Tsang, N. Zhu, *Inorg. Chem.* **2003**, *42*, 6886–6897.

[21] a) R. H. Wopschall, I. Shain, *Anal. Chem.* **1967**, *39*, 1514–1527; b) R. H. Wopschall, I. Shain, *Anal. Chem.* **1967**, *39*, 1527–1534.

[22] A. J. Bard, L. R. Faulkner, *Electrochemical Methods: Fundamentals and Applications*, 2nd ed., John Wiley & Sons, New York, **2001**.

[23] a) B. Schmid, F. O. Garces, R. J. Watts, *Inorg. Chem.* **1994**, *33*, 9–14; b) Y. Oshawa, S. Sprouse, K. A. King, M. K. DeArmond, R. J. Watts, *J. Phys. Chem.* **1987**, *91*, 1047–1054.

[24] M. Maestri, V. Balzani, C. Deuschel-Cornioley, A. v. Zelewsky, *Adv. Photochemistry* **1992**, *17*, 1.

[25] a) F. Neve, A. Crispini, S. Campagna, S. Serroni, *Inorg. Chem.* **1999**, *38*, 2250; b) I. M. Dixon, J. P. Collins, J. P. Sauvage, L. Flamigni, S. Encinas, F. Barigelletti, *Chem. Soc. Rev.* **2000**, *29*, 385–391.

[26] a) G. J. Barbante, C. F. Hogan, A. B. Hughes, *J. Solid State Electrochem.* **2009**, *13*, 599–608; b) G. J. Barbante, C. F. Hogan, A. Mechler, A. B. Hughes, *J. Mater. Chem.* **2010**, *20*, 891–899.

[27] C. Dragonetti, L. Falciola, P. Mussini, S. Righetto, D. Roberto, R. Ugo, A. Valore, *Inorg. Chem.* **2007**, *46*, 8533–8547.

[28] M. M. Cooke, E. H. Doeven, C. F. Hogan, J. L. Adcock, G. P. McDermott, X. A. Conlan, N. W. Barnett, F. M. Pfeffer, P. S. Francis, *Anal. Chim. Acta* **2009**, *635*, 94–101.

[29] V. Balzani, S. Campagna, G. Denti, A. Juris, S. Serroni, M. Venturi, *Coord. Chem. Rev.* **1994**, *132*.

[30] A. J. Bard, L. R. Faulkner, *Electrochemical methods: fundamentals and applications*, 2nd ed., John Wiley, New York, **2001**.

[31] J. Van Houten, R. J. Watts, *J. Am. Chem. Soc.* **1976**, *98*, 4853–4858.

[32] M. J. Frisch, G. W. Trucks, H. B. Schlegel, G. E. Scuseria, M. A. Robb, J. R. Cheeseman, G. Scalmani, V. Barone, B. Mennucci, G. A. Petersson, H. Nakatsuji, M. Caricato, X. Li, H. P. Hratchian, A. F. Izmaylov, J. Bloino, G. Zheng, J. L. Sonnenberg, M. Hada, M. Ehara, K. Toyota, R. Fukuda, J. Hasegawa, M. Ishida, T. Nakajima, Y. Honda, O. Kitao, H. Nakai, T. Vreven, J. J. A. Montgomery, J. E. Peralta, F. Ogliaro, M. Bearpark, J. J. Heyd, E. Brothers, K. N. Kudin, V. N. Staroverov, R. Kobayashi, J. Normand, K. Raghavachari, A. Rendell, J. C. Burant, S. S. Iyengar, J. Tomasi, M. Cossi, N. Rega, J. M. Millam, M. Klene, J. E. Knox, J. B. Cross, V. Bakken, C. Adamo, J. Jaramillo, R. Gomperts, R. E. Stratmann, O. Yazyev, A. J. Austin, R. Cammi, C. Pomelli, J. W. Ochterski, R. L. Martin, K. Morokuma, V. G. Zakrzewski, G. A. Voth, P. Salvador, J. J. Dannenberg, S. Dapprich, A. D. Daniels, Ö. Farkas, J. B. Foresman, J. V. Ortiz, J. Cioslowski, D. J. Fox, *Gaussian 09*, revision A02, Gaussian, Inc., Wallingford CT, **2009**.

[33] a) A. D. Becke, *Phys. Rev. A: Gen. Phys.* **1988**, *38*, 3098–3100; b) C. Lee, W. Yang, R. G. Parr, *Phys. Rev. B: Condens. Matter* **1988**, *37*, 785–789; c) A. D. Becke, *J. Chem. Phys.* **1993**, *98*, 5648–5652.

[34] a) C. Adamo, V. Barone, *J. Chem. Phys.* **1998**, *108*, 664–675; b) J. P. Perdew, in: *Electronic Structure of Solids '91* (Eds.: P. Ziesche, H. Eschrig), Akademie Verlag, Berlin, **1991**, pp. 11–20.

[35] a) W. J. Hehre, R. Ditchfield, J. A. Pople, *J. Chem. Phys.* **1972**, *56*, 2257–2261; b) T. Clark, J. Chandrasekhar, G. W. Spitznagel, P. v. R. Schleyer, *J. Comput. Chem.* **1983**, *4*, 294–301; c) P. C. Hariharan, J. A. Pople, *Theor. Chim. Acta* **1973**, *28*, 213–222.

[36] a) T. H. Dunning Jr, P. J. Hay, in: *Modern Theoretical Chemistry*, vol. 3 (Ed.: H. F. Schaefer III), Plenum, New York, **1976**, pp. 1–28; b) P. J. Hay, W. R. Wadt, *J. Chem. Phys.* **1985**, *82*, 270–283.

[37] J. Lin, K. Wu, M. Zhang, *J. Comput. Chem.* **2009**, *30*, 2056–2063.

[38] D. Andrae, U. Haeussermann, M. Dolg, H. Stoll, H. Preuss, *Theor. Chim. Acta* **1990**, *77*, 123–141.

[39] a) A. Schaefer, H. Horn, R. Ahlrichs, *J. Chem. Phys.* **1992**, *97*, 2571–2517; b) A. Schaefer, C. Huber, R. Ahlrichs, *J. Chem. Phys.* **1994**, *100*, 5829–5835.

[40] J. Tomasi, B. Mennucci, R. Cammi, *Chem. Rev.* **2005**, *105*, 2999–3093.

[41] R. E. Stratmann, G. E. Scuseria, M. J. Frisch, *J. Chem. Phys.* **1998**, *109*, 8218–8224.

[42] S. I. Gorelsky, *AOMix: Program for Molecular Orbital Analysis*, ver. 6.42, University of Ottawa, **2011**, http://www.sg-chem.net/.

Received: June 23, 2011
Published Online: September 22, 2011

